Technical Note:

Spectral slopes in deep, weakly-stratified ocean and coupling between sub-mesoscale motions and small-scale mechanisms

13

by Hans van Haren

20
21
22
23
24
25
26
27

30

31

Royal Netherlands Institute for Sea Research (NIOZ), P.O. Box 59, 1790 AB Den Burg, the Netherlands.
e-mail: hans.van.haren@nioz.nl

35
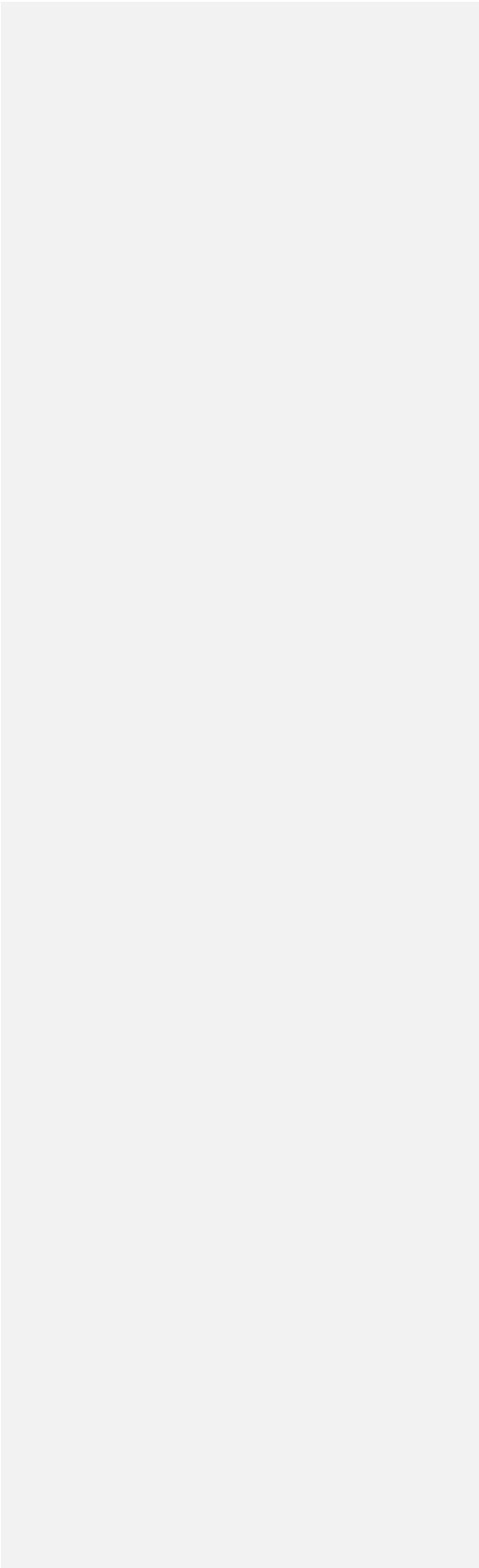
Short summary. Large ocean circulations include small-scale physical processes like transport by sub-mesoscale eddies and turbulence by internal wave breaking. Knowledge is lacking on precise interaction between different processes. In deep weakly stratified waters, continuous spectral slopes are observed that extend from sub-mesoscales across the internal wave band to turbulence range. Such cross-spectral correspondence is suggested a potential feedback mechanism stabilizing large-scale ocean circulations.

Abstract. Large, basin-wide ocean circulations are complex nonlinear dynamical systems. They include small-scale physical processes such as, for example, transport by sub-mesoscale eddies and turbulence-generating breaking of internal waves. To date however, knowledge is lacking on precise interaction between different processes. In this note, a potential contributor to interaction is investigated using spectra from deep-sea moored observations. In weakly stratified waters, continuous spectral slopes are observed that extend from sub-mesoscales across the internal wave band to turbulence range. In the latter, the governing slope can be distinctly different from the inertial subrange of shear turbulence and is described as the buoyancy subrange of convection turbulence. At sub-inertial frequencies, the slope's extension either describes quasi-gyroscopic waves or sub-mesoscale eddies. Such cross-spectral correspondence is suggested a potential feedback mechanism stabilizing large-scale ocean circulations.

1 Introduction

The extent of anthropogenic influence on the Earth's climate warrants studies of the ocean as a major player. Large, basin-wide ocean circulations are important for transporting properties like heat, carbon and nutrients. Schematically, the Atlantic(-Ocean) Meridional Overturning Circulation (AMOC) is depicted to transport heat from the equator to the poles near the surface and carbon in the abyssal return (e.g., Aldama-Campino et al., 2023). It includes physical processes like 'deep dense-water formation' in the polar region. Recent mathematical and numerical modelling such as based on varying single parameters like sea-

64   surface temperature (e.g., Ditlevsen and Ditlevsen, 2023) and freshwater influx (e.g., van

65   Westen et al., 2024) suggest a potential future collapse of the AMOC. It is argued that this

66   may have consequences for Northwest-European climate.

67   Whilst the modelling might be robust mathematically, it lacks physical processes of

68   the drivers of the AMOC and observational evidence thereof. This will have consequences for

69   the feedback mechanisms at work in the nonlinear dynamical system of ocean circulation. As

70   has been reviewed for AMOC numerical models (Gent, 2018), important feedback

71   mechanisms are vertical turbulent mixing, sub-mesoscale gyre 'eddy' transport, and the

72   coupling with the atmosphere. Here we elaborate on the importance of turbulence induced by

73   internal wave breaking, possibly coupling with sub-mesoscale eddies (e.g., Chunchuzov et al.,

74   2021), and stability variations in vertical density stratification for such feedback, by

75   reviewing insights from recent modeling and deep-sea observations. In particular as an

76   example for complexity of dynamical system interactions, the core of ocean motions is

77   spectrally investigated focusing on most energetic mesoscale, internal wave, and turbulence

78   scales, for deep weakly stratified waters.

79   In contrast with the atmosphere, the ocean is not an effective heat engine (Wunsch

80   and Ferrari, 2004) despite its heat transportation. As a result, the AMOC is not predominantly

81   buoyancy-driven via push by deep dense-water formation near the poles (Marshall and Schott,

82   1999; Marotzke and Scott, 1999), which notably occurs in sporadic pulses rather than

83   continuously. Instead, the AMOC is mainly wind-steered (e.g., Liu et al., 2024) and tide-

84   driven, with turbulent mixing by internal wave breaking, and possibly associated upwelling

85   close to boundaries (Ferrari et al., 2016; McDougall and Ferrari, 2017), being considered an

86   important physics process of pull that dominates over push by a heat engine. Winds, near the

87   ocean surface, and tides, via interaction with seafloor topography deeper down, contribute

88   about equally to generate internal waves that are found everywhere in the ocean interior. Such

89   waves break predominantly at ubiquitous underwater seamounts and continental slopes.

90   Without turbulent mixing, the AMOC would be confined to a 100-m thick near-

91   surface layer and the deep-ocean would be a stagnant pool of cold water (Munk and Wunsch,

92   1998). This is not the case however, and the solar heat is mixed from the surface downward

93   so that the ocean is stably stratified in density all the way into its deepest trenches, as has been

94   shown in hydrographic deep-ocean observations (Taira et al., 2005; van Haren et al., 2021a).

95   Although turbulent mixing by internal wave breaking in the ocean-interior is insufficient by at

96   least a factor of two to maintain the vertical density stratification (e.g., Gregg, 1989, Polzin et

97   al., 1997), such breaking along ocean boundaries has been suggested to be more than

98   sufficient (Munk, 1966; Polzin et al., 1997). Especially large internal wave breaking is

99   expected to occur above steeply sloping topography (Eriksen, 1982; Thorpe, 1987; Sarkar and

100   Scotti, 2017). Because there are more and larger seamounts than mountains on land, equally

101   abundant sloping seafloors lead to abundant turbulent mixing, as has been charted from recent

102   observations and modelling results summarized below.

103   As recent observations (van Haren and Dijkstra, 2021; van Haren et al., 2024)

104   demonstrate that breaking waves can lead to considerable buoyancy driven convection

105   turbulence, this note attempts further understanding of a little studied deep-sea complex

106   process and its potential interaction with sub-mesoscale motions. The sub-inertial range of

107   sub-mesoscale motions has rarely been a subject of oceanographic spectral observations.

108   Knowledge about such small-scale processes and their interactions may be vital for

109   understanding potential feedback mechanisms affecting the stability of large-scale ocean

110   circulations.

111

112   **2 Recent internal wave breaking results**

113   Detailed observations and numerical modeling have revealed the extent of internal

114   tide breaking processes above ocean topography (van Haren and Gostiaux, 2012; Winters,

115   2015; Wynne-Cattanach et al., 2024). Using high-resolution observations (e.g., van Haren and

116   Gostiaux, 2012), internal tide breaking above steep deep-sea slopes is observed to generate

117   spring-neap-average turbulent vertical diffusivity value of about 3×10^{-3} m^2 s^{-1}. This value is

118   twice the value theoretically required to yield upwelling in a thin layer above sloping

119   topography (McDougall and Ferrari, 2017). Such quantification of turbulent mixing shows

120 that it occurs with typical tidal-period-average values that are more than 100 times larger over

121 super-critical slopes than open-ocean values. A super-critical seafloor slope is steeper than the

122 slope of internal wave characteristics. While ocean-wide tides energetically dominate internal

123 waves, not all seafloor slopes are super-critical for these waves. In contrast, nearly all seafloor

124 slopes are super-critical for at least one component of secondary energetic near-inertial

125 waves, which are generated via geostrophic adjustment following the passage or collapse of a

126 disturbance such as fronts or atmospheric storms on the rotating Earth. Under common

127 stratification, near-inertial waves are at the lowest frequency of freely propagating internal

128 waves. The highest frequency propagating internal waves, near the buoyancy frequency,

129 experience nearly vertical walls as super-critical seafloor slopes.

130   Within a tidal, or near-inertial, period, turbulence peaks in bursts of shorter duration

131 than half an hour when highly nonlinear internal waves propagate as internal bores up a

132 super-critical slope, once or twice a tidal cycle. The breaking of bores leads primarily to

133 convection, buoyancy-driven turbulence, rather than frictional shear-turbulence over the

134 sloping seafloor and occur at a wide variety of deep-sea and deep-ocean locations (e.g., van

135 Haren et al., 2013; van Haren et al., 2024). Between bores, the turbulent mixing varies by an

136 order of magnitude in intensity, with effects extending about 100 m vertically and several

137 kilometers horizontally from the seafloor. Although intermittently occurring at a given

138 position of the sloping seafloor and about 10% varying in arrival time, the turbulence is

139 generated internally by the tide, for about 60% (Wunsch and Ferrari, 2004), and by winds, for

140 about 40%, in a stratified ocean-environment. The turbulent bores also resuspend sediment

141 and thereby replenish nutrients away from the seafloor (Hosegood et al., 2004), important for

142 deep-sea life. Enhanced turbulent mixing above sloping boundaries has a demonstrated effect

143 on the outcome of general ocean circulation models (e.g., Scott and Marotzke, 2002), with

144 predicted subtle effects on upwelling near the seafloor (Ferrari et al., 2016).

145   The complexity of turbulence generation, mixing and restratification, are still subjects

146 of deep-ocean research. While shear-induced turbulence has been relatively well studied in

147 the stratified ocean, deviations such as convection-turbulence are little observed, with recent

148 exceptions (van Haren and Dijkstra, 2021; van Haren et al., 2024). Convection turbulence is

149 dominant in the atmosphere especially during daytime, and has also been observed in the

150 near-surface ocean during nighttime (e.g., Brainerd and Gregg, 1995), but it has never been

151 quantitatively directly observed in deep dense-water formation zones (Thorpe, 2005) and

152 above geothermal vents. Lagrangian float measurements yielded average vertical heat flux

153 estimates due to convection reaching down to 1000 m from the surface in the Labrador Sea

154 (Steffen and D'Asaro, 2002). It would be challenging to set-up an experiment in which such

155 floats are equipped with microstructure instrumentation, and be able to measure convection

156 turbulence from the surface down to the deep seafloor.

157   Deep dense-water formation does not only occur in polar seas, but occasionally also

158 in the at least 10°C warmer Mediterranean (Gascard, 1978), with an important contribution of

159 atmospheric exchange due to orographic generated winds affecting the preconditioning by

160 cooling and drying of near-surface waters. Similarly, internal waves occur in oceans and in

161 the Mediterranean under stratification conditions that vary over at least one order of

162 magnitude in time and space, but tides are relatively weak in the Mediterranean, and yet

163 'sufficient' turbulent diapycnal mixing, sufficient for maintenance of deep-sea stratification

164 and thereby driving overturning circulation, is generated via the breaking above topography

165 of near-inertial motions mainly (van Haren et al., 2013). Further complications are expected

166 from interactions of internal waves with sub-mesoscale eddies and potential consequences of

167 varying intensity thereof, e.g., on seasonal scales.

168

169 **3 Mediterranean observations as an example proxy for ocean conditions**

170   In many physical oceanographic aspects of heat and salt budgets, large-scale water-

171 flow circulation, strong boundary flow, eddies at sub-mesoscales, near-inertial motions

172 including gyroscopic waves and internal wave turbulence, the Mediterranean Sea can be

173 considered a sample for the state of the much larger oceans (e.g., Gascard, 1973; Crepon et

174 al., 1982; Garrett, 1994; Milllot, 1999; van Haren and Millot, 2004; Testor and Gascard,

175   2006). Like in oceans, the Mediterranean seafloor reaches great depths and can be rugged

176   with steep slopes in places, including continental slopes incised by deep canyons.

177   In the Northwest Mediterranean, vertical density stratification varies markedly with

178   seasons and years, having relatively large near-surface values in summer and relatively low

179   values in winter. The proximity of extensive mountain ranges on land generates highly

180   variable winds that can cool and dry surface waters. In winter in weaker stratified waters, this

181   may lead to unstable conditions of buoyancy driven convection in an exchange of dense-water

182   sinking down, and less dense-waters up. Like in the polar regions, such exchange can be

183   observed daily in the upper 10 m from the sea-surface, regularly down to a few 100 m from

184   the surface, and seldom, once every 5-8 years (e.g., Rhein, 1995; Mertens and Schott, 1998),

185   down to the abyssal seafloor at about 2500 m. In contrast, horizontal density gradients

186   associate with forcing of a dynamically unstable boundary current and eddies at multiple 1-

187   100 km sub-mesoscales (e.g., Crepon et al., 1982; Testor and Gascard, 2006). These eddy

188   motions may push relatively warm waters down, thereby increasing the weak stratification in

189   the deep-sea.

190   In summer, atmospheric disturbances are less intense, near-surface stratification is

191   large due to solar heating, and eddy activity associated with some continental boundary flows

192   is weaker (Albérola et al., 1995). This opens the possibility for detection of near-inertial wave

193   dominance in kinetic energy. In relatively strong stratification, mainly gravity-driven parts of

194   near-inertial waves generate largest vertical current differences 'shear' that destabilize

195   stratification due to their relatively short vertical length-scale, not only in the Mediterranean

196   but also as observed in the Atlantic Ocean (van Haren, 2007). This destabilization may lead to

197   small-10-m vertical scale layering of near-homogeneous waters throughout seas and oceans.

198   On larger-100-m vertical scales near-homogeneous waters occur in deep waters of the

199   Mediterranean as well as of North-Atlantic basins like the Bay of Biscay and Canary Basin.

200   In near-homogeneous water-layers with weak stratification, gyroscopic, Earth-rotation-driven,

201   parts of near-inertial waves dominate and result in 0.1-1 km diameter smaller than sub-

202   mesocale tubes of slantwise rather than vertical convection (Emanuel, 1994; Marshall and

203 Schott, 1999; van Haren and Millot, 2004). Hence, one may expect frequency spectra of non-

204 tidal dominated data from instruments moored in the Mediterranean reveal convection and

205 thus deep transport under winter and summer conditions.

206   It is noted that ocean-spectra, such as frequency spectra of kinetic energy and scalar

207 quantities like temperature from data registered by moored instrumentation, may show peaks

208 such as at narrowband tidal and at, broader band, inertial frequencies, but they lack gaps. This

209 lack of spectral gaps potentially couples motions at sub-inertial with inertial-buoyancy

210 internal wave with super-buoyancy turbulence frequency ranges. However, it is unclear how

211 such a coupling may work as some motions represent two-dimensional '2D' eddies, some

212 linear waves, some non-linear waves, some anisotropic, quasi 3D, stratified turbulence, and

213 some isotropic 3D turbulence. This is investigated by renewed spectral analysis below, using,

214 in analogy, slopes typical for investigating energy cascades in turbulence research.

215

216 **4 Uncommon slopes in revisited spectra**

217   Kinetic energy (KE) spectra from historic moored current meter observations down to

218 mid-depth $z = -1100$ m in the Ligurian Sea under upper-sea strongly stratified 'summer' and

219 weakly stratified 'winter' conditions surely lack gaps (Fig. 1). Year-round at $z = -1100$ m, the

220 buoyancy frequency N, reflecting the square-root of vertical density stratification, is small N

221 $\sim O(f)$, f denoting the inertial frequency involving Earth rotation. This narrows the local

222 internal wave band, while, especially in winter, sub-mesoscale activity is large in the area,

223 and, occasionally, the few moored current meter temperature records showed inversions (van

224 Haren and Millot, 2003). Although these hourly sampled data barely resolve the turbulence

225 ranges at frequencies $\omega > N$, the internal wave continuum was suggested to scale like ω^p,

226 with, on a log-log plot, 'spectral slope' $p = -2.2\pm0.4$, independent of location and season

227 albeit with different KE (power) levels.

228   Within the uncertainty range, several possible explanations can be given for the

229 observed spectral slope. Freely propagating internal gravity waves have been fitted to $p = -$

230 2±0.5 but only for f << ω << N (Garrett and Munk, 1972). Considering that the data in Fig. 1

231 are from a site where locally N = (3±2)f, irrespective of season (van Haren and Millot, 2003),

232 alternative explanations were sought for observed spectral slopes at sub-inertial frequencies

233 0.2 cpd < ω < f. Cpd is short for 'cycles per day'. An obvious candidate is 'fine-structure

234 contamination' of step functions passing sensors, which gives a theoretical vale of p = -2

235 (Phillips, 1971; Reid, 1971). For their winter data, van Haren and Millot (2003) attributed

236 such a slope to evidence intense mesoscale activity, because of the continuation of slope up to

237 ω = 5 cpd before rolling off near the Nyquist frequency. However, they did not elaborate.

238 Below, the data in Fig. 1 are re-analyzed from the perspective of convection-turbulence.

239   Theoretical considerations of non-zero-mean flow convection-turbulence suggest a

240 spectral scaling in the buoyancy subrange having p = -11/5 = -2.2 for KE, and p = -7/5 for an

241 active scalar quantity. This 'BO'-scaling follows atmospheric and theoretical works by

242 Bolgiano (1959) and Obukhov (1959). The scaling was set-up for a stably stratified

243 atmospheric environment for the anisotropic part in which turbulent kinetic energy is partially

244 transferred to potential energy leading to turbulent convection. Later works extended BO-

245 scaling to purely buoyancy-driven turbulence, e.g., for Rayleigh-Bénard convection (Lohse

246 and Xia, 2010) and Rayleigh-Taylor instabilities (Poujade, 2006; Celani et al., 2006).

247   Laboratory experiments on such gravitationally driven convection are inconclusive on

248 BO-scaling. On the one hand, this scaling is confirmed for both KE and temperature in

249 experiments by Ashkenazi and Steinberg (1999), while on the other hand it is only confirmed

250 for scalars by Pawar and Arakeri (2016) who found a slope of p = -5/3 for KE. The p = -5/3-

251 slope suggests dominance of shear-induced turbulence of the inertial subrange for equilibrium

252 isotropic turbulence cascade in the 'KO'-scaling (Kolmogorov, 1941; Obukhov, 1949) but

253 should also be found in spectra of scalars that are passive in this range. While Liot et al.

254 (2016) show KO-scaling in their model that may have to do with their Lagrangian data as

255 proper transfer brings the data closer to BO-scaling, Poujade (2006) and Cenari et al. (2006)

256 show clear BO-scaling in their models. This suggests particular conditions do affect the

257 dominance of shear- or convection-turbulence. It is noted that BO-scaling is also simply

258 considered as a significant deviation from KO-scaling, which is more commonly observed in

259 stratified shear flows.

260 Obviously, scalars cannot be passive and active at the same time and in the same

261 space. This discrepancy between types of scaling between scalars and KE may be because the

262 laboratory experiments of Pawar and Arakeri (2016) were in zero mean flow. Also, under

263 sufficiently stable conditions without shear, no inertial subrange is expected (Bolgiano, 1959).

264 However, the spectral extent of BO-scaling is largely unknown albeit it is more generally

265 found adjacent to higher-frequency inertial subrange. While KO-scaling is based on a forward

266 cascade of energy, the direction of energy cascade is inconclusive for BO-scaling and may be

267 partially forward and partially backward, at least as reasoned for pure buoyancy-driven

268 convection-turbulence (Lohse and Xia, 2010). Probably, directions of cascade change with

269 locality in the flow, and perhaps depend on scale, which would also imply that KO- and BO-

270 scaling cannot be found at the same site.

271 Revisiting data from non-zero mean flow and weakly stratified deep-sea in Fig. 1

272 demonstrates the possibility of fit of $p = -11/5$ outside near-inertial harmonic peaks. In winter,

273 such a fit is observed consistently through the entire range of $0.2 < \omega < 5$ cpd. In traditional

274 terms, this frequency range covers the transition from mesoscale $\omega < f$, via internal wave $f <$

275 $\omega < N$, to turbulence $\omega > N$ motions. In summer, the $p = -11/5$-slope is found at two different

276 KE levels for bands $0.2 < \omega < \omega_{min}$ and $2\Omega < \omega < 5$ cpd at sub- and super-IGW frequencies,

277 respectively. Here, $\omega_{min} \leq f$ denotes the minimum frequency bound for inertio-gravity waves

278 IGW (LeBlond and Mysak, 1978), and Ω the Earth rotational frequency. Maximum IGW

279 frequency is denoted by $\omega_{max} \geq 2\Omega$, N. The ω_{min} and ω_{max} are functions of N, latitude φ and

280 direction of wave propagation (LeBlond and Mysak, 1978; Gerkema et al., 2008),

281 $\omega_{max}, \omega_{min} = (A \pm (A^2-B^2)^{1/2})^{1/2}/\sqrt{2}$,   (1)

282 in which $A = N^2 + f^2 + f_s^2$, $B = 2fN$, and $f_s = f_h sin\alpha$, α the angle to φ. For $f_s = 0$ or $N \gg 2\Omega$,

283 the traditional bounds [f, N] are retrieved from (1). The plotted IGW-bounds [ω_{min} ω_{max}] are

284   for weakly stratified, near-homogeneous layers in which $N = f$. This weak stratification would

285   lead to an impossible wave solution under the traditional approximation, but (1) allows wave

286   propagation, albeit horizontally for one component (e.g., Gerkema et al., 2008).

287   The bridge between the KE-levels at sub- and super-IGW is formed by the finitely

288   broad near-inertial peak. The base of this peak is proposed to slope like $p = -1$ reaching super-

289   IGW BO-scaling at about $\omega \approx 4$ cpd $\approx N$. Such $p = -1$-slope has been observed for the KE-

290   spectral continuum between $[f \; N]$ from the deep Bay of Biscay, Northeast Atlantic Ocean

291   (van Haren et al., 2002). Theoretically, this slope represents spectral scaling of intermittency

292   of a weakly chaotic nonlinear system (Schuster, 1984), i.e., 3D dynamical systems that evolve

293   into self-organized critical structures of states which are minimally stable (Bak et al., 1987).

294   Such a spectral bridge, or hump, is expected for turbulence in unstable stratification, as has

295   been illustrated using atmospheric observations (Lin, 1969). It is attributed to the flow field

296   absorbing energy from the scalar temperature field as potential energy is transferred to kinetic

297   energy. It is not clear to what extent near-inertial internal waves contribute in a similar way to

298   spectral redistribution of energy in our oceanographic data. As the observations from the

299   central Ligurian Sea show similar results, the hump is unlikely associated with seafloor slopes

300   matching the slope of near-inertial internal wave rays.

301   These spectral observations suggest a dominance of convection cascade from sub-

302   meso- via IGW- to, probably because unresolved, turbulence-scales under high-energetic

303   winter-conditions as they show a continuous slope across their frequency ranges. Such a

304   cascade is also suggested under quieter summer conditions when, however, it is masked by

305   IGW that lead a cascade at $\omega > \omega_{min}$. Especially the sub-inertial range of apparent BO-scaling

306   seems out of the turbulence range, unless waters are near-homogeneous $N \rightarrow 0$ so that $\omega_{min} \rightarrow$

307   0, from (1). This would extend not only IGW, notably gyroscopic waves, but also turbulence,

308   probably in the form of slantwise convection, to the sub-mesoscale range.

309   For the mesoscale range, the observations in Fig. 1 are supported by numerical

310   modeling results that have suggested eddy-KE has a broad range of spectral slopes between -3

311   < p < -5/3 (Storer et al., 2022), and by satellite altimetry observations that indicated, after

312   noise-correction and transfer to KE, a best-fit of p = -2.28 (Xu and Fu, 2012). No mention

313   was made of BO-scaling, but the correspondence seems evident.

314   As the KE in Fig. 1 is at least one order of magnitude larger in winter than in

315   summer, a near-inertial peak, if it exists, will be part of the spectral continuum during the

316   former. The winter observations suggest a continuous spread of sub-mesoscale energy across

317   the IGW band including inertial motions and into the turbulence range. In winter, near-surface

318   stratification is considerably weaker than in summer, so that local atmospheric-generated

319   near-inertial motions will be smaller. It is noted that the signals near the Nyquist frequency

320   not only contain instrumental white noise, but also unresolved turbulence motions, which are

321   also larger in winter than in summer.

322   Inspired by Western Mediterranean observations, Saint-Guily (1972) proposed from

323   theoretical work that winter-time inertial KE is spread over a broad featureless band, like

324   quasi-gyroscopic waves that may be present between IGW-bounds (1) for $N \sim f$ (LeBlond and

325   Mysak, 1978; Gerkema et al., 2008). However, observations from the year-round upper-layer-

326   stratified central Western Mediterranean demonstrate that, also in deep homogeneous $N = 0$

327   waters, a near-inertial peak can be observed in KE-spectra (van Haren and Millot, 2004). This

328   may be attributed to a year-round source of atmospheric-generated inertial waves that are the

329   only internal waves that can propagate without attenuation from well-stratified to near-

330   homogeneous layers and vice versa (van Haren, 2023b).

331   Based on limited spectral observations, Gascard (1973) suggested the generation of

332   12-h stability waves, close to the buoyancy frequency of very weak stratification, which may

333   briefly force dense-water formation, thereby implicitly suggesting a link between internal

334   waves and sub-mesoscale eddies. As such eddies have estimated relative vorticity of $|\zeta| = f/2$

335   in the Western Mediterranean (Testor and Gascard, 2006), this addition to the planetary

336   vorticity (f) automatically widens the 'effective' near-inertial band $0.5f < f_{eff} < 1.5f$, of which

337   the bounds are close to IGW-bounds for $N = 0.8f$. One of the properties can be a modification

338   of near-inertial frequency (Perkins, 1976), and trapping with downward propagation of near-

339   inertial waves in anticyclonic eddies (Kunze, 1985; Voet et al., 2024). Such frequency

340   modification may add to local physics of inertial wave caustics due to latitudinal variation

341   (LeBlond and Mysak, 1978), which however can only lead up to 15% change in f in the

342   Mediterranean. Although found to be limited to the rather flat KE-spectral dip in the

343   immediate half-order-of-magnitude sub-inertial frequency band, standing vortical modes, i.e.

344   low-frequency non-propagating motions, of vertical length-scale <10 m are suggested to be as

345   energetic as internal waves (Polzin et al., 2003). Alternatively, it has been suggested for

346   North-Atlantic observations that vortical modes may interact with internal waves, affecting

347   internal-wave shear that was peaking over O(10) m vertical scales at IGW-frequencies in a

348   band with limits determined by weak stratification as in $N = f$ (van Haren, 2007).

349   For hypothetical ω_{min} = 0.2 cpd, at which the observed spectral slope changes away

350   from p = -11/5 (Fig. 1), one would require $N = 0.21f$, which is almost unmeasurable and non-

351   existent for any prolonged period even in the deep Northwestern Mediterranean, to the

352   knowledge of the author. However, it may reflect ω_{min} computed using $f_{eff} = 0.5f$ and $N = f_{eff}$,

353   noting that such conditions can only apply for part of the record. If so, it would reflect a direct

354   coupling between sub-mesoscale and IGW-motions with slantwise convection (Marshall and

355   Schott, 1999; van Haren and Millot, 2004; Gerkema et al., 2008). The p = -11/5 is

356   significantly distinguishable from -2 over a frequency range of nearly two orders of

357   magnitude, and from -5/3 over a range of just over half an order of magnitude (Fig. 1). The

358   roll-off to noise (slope 0), for ω > 5 cpd, may partially be seen as following a slope of p = -5/3

359   before 0. The roll-off around 0.1 cpd suggests an unresolved broad mesoscale peak-value

360   between 0.01 and 0.1 cpd. While these 1980's moored current meter data barely resolved the

361   turbulence part of the KE-spectrum, and thus also not the p=-5/3 inertial subrange slope, their

362   temperature sensors were too poor to simultaneously verify any spectral scaling for scalars.

363   About 40 years later, high-resolution and high-precision moored temperature sensor

364   'T-' data provided opportunity to verify scalar spectral scaling of turbulence energetic

365   motions in the area. These T-data evidenced occasional warming of the deep Northwest

366   Mediterranean seafloor (Fig. 2a), which, after comparison with data from higher-up appeared

367   to be coming from above, or slanted sideways, under relatively stratified conditions, and from

368   general non-vents geothermal heating from below (van Haren, 2023a). The data were

369   collected during mid-fall, when near-surface waters were well stratified and no cold, dense-

370   water production through convection was observed. Locally near the seafloor, the broad two-

371   day warming around day 308 is most stratified, whilst during other periods waters are only

372   weakly stratified, including the quasi-inertial variations between days 316 and 322. These

373   weakly stratified near-inertial, or near-buoyancy as N ≈ f, temperature variations may

374   evidence slantwise quasi-gyroscopic near-inertial waves, which can have a large vertical

375   component (LeBlond and Mysak, 1978), as opposed to more common near-horizontal near-

376   inertial waves in strongly stratified waters that are barely noticeable in temperature records.

377   The 18-day average spectrum of the 2-s sampled data poorly resolves sub-mesoscales

378   but shows, near the seafloor, a well-resolved slope of $p = -1.4\pm0.025$ between a large range of

379    $0.5 < \omega < 6000$ cpd, across the IGW band and well into the turbulence band (Fig. 2b). No

380   transition to a -5/3-slope is observed before roll-off to noise, but this does not exclude an

381   inertial subrange at higher frequencies hidden under white noise, although shear will be

382   limited so close to the seafloor. The observed $p = -7/5$-slope is found significantly different

383   from $p = -2$ and -5/3 over the indicated frequency range of four orders of magnitude and over

384   the range between $100 < \omega < 10^4$ cpd thereby representing convection turbulence. Over a

385   frequency range of half an order of magnitude the slope-error is about ±0.1. Albeit not greatly

386   resolved, the range between $\omega_{max} < \omega < 10$ cpd falls-off more steeply roughly at $p = -2$ and the

387   range between $10 < \omega < 100$ cpd shows a reduced variance that may partially be characterized

388   by intermittency ($p = -1$; Schuster, 1984), but which is not yet explained. Here, it is observed

389   to bridge between $p = -2$ and super-IGW BO-scaling $p = -7/5$. This would be further

390   observation of a marginally ocean-state to the -1-scaling in KE-spectra (present Fig. 1 and van

391   Haren et al., 2002) and in the continuum of the band [f N] in open-ocean T-spectra (van

392   Haren and Gostiaux, 2009).

393   About 140 m above the seafloor, a less precise older-type T-sensor demonstrates p = -
394   7/5 between a reduced range of about $10 < \omega < 1000$ cpd, with a suggestion for p = -5/3
395   around 10 cpd. This indicates convection can still dominate over shear extending O(100 m)
396   above the seafloor, as has been shown in more detail for certain periods (van Haren, 2023c).

397   Whilst more extended work with longer data sets and more T-sensors is to be done,
398   the extended continuous spectral slope from these high-resolution temperature observations
399   suggests a direct coupling between sub-mesoscale motions, IGW motions, comprising
400   internal gravity and gyroscopic waves, and convection turbulence. The temperature spectra
401   also show consistency with the limited KE-spectra of Fig. 1 from roughly the same area, and
402   both indicate a dominance of non-isotropic, stratified-turbulence convection between sub-
403   mesoscales and largest turbulent overturning scales in extended BO-scaling suggesting cross-
404   spectral coupling. The discrepancy with KE-spectra in laboratory experiments of Pawar and
405   Arakeri (2016) may be due to the difference of settings. In a non-zero-mean flow turbulence
406   convection experiment near the gas-liquid critical point, BO-scaling was observed for both
407   KE and temperature (Ashkenazi and Steinberg, 1999). We recall that our deep-sea conditions
408   are non-zero-mean flow, weak tides, very high bulk Reynolds numbers $O(10^5)$ given the large
409   scales, varying non-zero vertical density stratification, and our example spectra did not clearly
410   resolve KO-scaling.

411   This 18-day T-sensor data set demonstrates dominant deviations from inertial
412   subrange over several orders of magnitude of frequency range. The mesoscale-IGW-
413   turbulence motions transport and locally mix warm waters with cooler surroundings outside a
414   period of buoyancy-driven dense-water formation, which is thought to bring cooler waters
415   downward during short periods of time.

416

417   **5 How robust is the system of ocean circulation and stratification?**

418   Any variation to the nonlinear system of ocean circulation may encounter several
419   complex feedback mechanisms, of which the effects are not yet fully understood for the
420   present-day ocean. Although stable density stratification hampers vertical exchange by

421 turbulent mixing, it does not block it. While stratification supports internal waves and their

422 destabilizing shear, turbulent mixing during particular phase of a wave may decrease or

423 destroy it locally in time and space. However, a subsequent internal wave-phase will restratify

424 the mixed patch, thereby maintaining its own support of stable stratification. Such a feedback

425 system may be at work, for example when the ocean absorbs more heat.

426 Increased sea-surface temperature may lead to increased vertical density

427 stratification, which may lead to less turbulent exchange as vertical overturning is suppressed.

428 However, it will also lead to more internal waves through the extension of their spectral band

429 to higher frequencies, with the potential to increased interaction, non-linearity, and

430 turbulence-generating wave breaking. As particular internal waves can propagate deep into

431 the ocean interior away from their source, they can cause enhanced turbulent mixing

432 elsewhere (e.g., Alford, 2003).

433 Limited observations have thus far not provided evidence for an inverse

434 correspondence between changes in turbulent mixing and changes in temperature across the

435 near-surface photic zone along a longitudinal section of the Northeast Atlantic Ocean (van

436 Haren at al., 2021b). This lack of correspondence suggests a feedback mechanism at work

437 mediating potential physical environment changes so that global warming may not affect

438 vertical turbulent fluxes of heat, and thereby also of, e.g., carbon.

439 One such feedback mechanism may be convection-turbulence induced by internal

440 waves and sub-mesoscale eddies. Renewed analysis of yearlong moored current meter data

441 from the Irminger Sea, North-Atlantic Ocean, demonstrate a significant $p = -11/5$ spectral

442 slope at sub- and at super-inertial frequencies (Fig. 3). As was outlined in van Haren (2007),

443 the area showed an IGW-band (1), for $N = f$, with dominant sub-inertial shear at small 8-m

444 vertical scales despite the dominant internal tidal KE. The correspondence with the

445 Mediterranean data of Fig. 1 is striking, including the one order of magnitude change in KE

446 between sub- and super-IGW $p = -11/5$-slopes with similar $p = -1$ bridge albeit uncertain

447 crossing level, and similar heights of near-inertial peak despite the tidal peak in Fig. 3.

Moored deep-water observations (e.g., van Haren and Dijkstra, 2021; van Haren et al., 2024) have demonstrated BO-scaling at internal wave-turbulence frequencies smaller than the Ozmidov frequency, the largest scale at which isotropic 3D turbulent overturns can exist in a stratified environment. This bears similarity with 'stratified turbulence' having low Froude numbers at horizontal scales O(10-100) m exceeding the Ozmidov scale, and which includes nonlinear internal waves (Riley and Lindborg, 2008; Falder et al., 2016; Chini et al., 2022). Horizontal wavenumber k_h-spectra are presented arguing that a scaling of $k_h^{-5/3}$ in fact reflects stratified turbulence outside the inertial subrange of isotropic 3D-turbulence. However, visual inspection also shows BO-scaling in several figures of Riley and Lindborg (2008). As the internal wave/turbulence range is associated with vertical Froude numbers O(1), stratified turbulence has been associated with 'marginal stability' in numerical modelling (Chini et al., 2022). Previously, marginal stability was described in the context of nonlinear flows (Abarbanel et al., 1984) and, e.g., explaining stratified North-Sea observations (van Haren et al., 1999).

While few ocean observations have been presented of BO-scaling thus far in comparison with KO-scaling, perhaps also because of the lack of precision of standard oceanographic instrumentation, coupling has not been established between convection and stratified small-scale turbulence with mesoscale motions. Likewise, complicating factors are spectral interruption by internal waves. However, internal wave trapping by mesoscale eddies has been well described (e.g., Kunze, 1985; Voet et al., 2024), and thus provides an obvious coupling between these motions. It is expected that such coupling may lead to strong nonlinearity of the internal waves that leads to turbulent mixing produced by wave breaking. Although such turbulent mixing is smaller than that induced by internal wave breaking above sloping topography, such coupling may be an important factor in downward transport of near-inertial energy that eventually breaks elsewhere, e.g., over topography.

As demonstrated using Mediterranean observations, not only convectively unstable cooler and/or saltier waters potentially lead to downward motions from the surface. Also, sub-mesoscale eddies and near-inertial waves can push stratified waters to the deep sea. Such a

476 downward push can be fast to transport materials from surface to 2500-m deep seafloor in a

477 day (van Haren et al., 2006), and which is of the same order of magnitude as attributed to

478 dense-water convection (Schott et al., 1996). It can also be more turbulent compared to shear-

479 induced motions in the stratified ocean-interior, whereby turbulence reaches the seafloor

480 according to few observations from the abyssal Pacific (van Haren, 2020) and alpine

481 freshwater Lake Garda (van Haren and Dijkstra, 2021). Further extended observational

482 evidence is urgently needed, preferably resolving much larger scales.

483   Although the anthropogenic influence on the Earth's climate is without doubt, the

484 impact on ocean circulation is not fully known because we lack sufficient, notably

485 observational, information of the relevant processes that thus cannot be properly modeled yet.

486 Therefore, we should be cautious in making predictions (e.g., Ditlevsen and Ditlevsen, 2023;

487 van Westen et al., 2024) on future ocean circulation based on single parameters like ocean-

488 surface temperature or fresh-water flux that are uncertain proxies. Because no observational

489 (van Haren et al., 2021b), modeling (Little et al., 2020) or paleo-proxy validation (Cisneros et

490 al., 2019) physics evidence exists that sea-surface temperature is a solid estimator of AMOC-

491 strength variations, other properties like vertical density gradients (stratification), and

492 turbulence intensity may be considered. Small-scale physical processes such as, for example,

493 transport by sub-mesoscale eddies and turbulence-generating breaking of internal waves that

494 are not incorporated in these models will alter such parameters, and thereby statistical

495 analyses. This may lead to feedback mechanisms on property gradients such as density

496 stratification so that large-scale ocean circulations like the AMOC may not collapse.

497   Variability of the ocean in space and time is a key to its dynamics, but it is unclear

498 how robust such variations can be, e.g., whether shifting sites for deep dense-water formation

499 (Gou et al., 2024) may be part of the same system. Observational evidence verifying

500 numerical simulations' outcome, not only predictions but also present-day, of ocean-state is

501 needed. Observations are also required to demonstrate variability in relevant physics

502 processes for model-implementation. Besides eddies and coupling with atmosphere (e.g.,

503 Gent, 2018), numerical models of complex nonlinear ocean circulation should contain

504 internal-wave turbulence with appropriate space and time dependency. The importance of
505 internal wave breaking leading to boundary mixing above sloping topography in general
506 ocean circulation models has been acknowledged in various ways (Scott and Marotzke, 2002;
507 Ferrari et al., 2016).

508 As for the ocean circulation in the horizontal plane near its surface with most impact
509 on mankind, wind will remain the main driver. As long as the Earth rotation does not alter
510 direction, wind will maintain its general course (Wunsch, 2004). The atmosphere remains the
511 key player in the global heat transport across mid-latitudes rather than the ocean.
512 Simultaneously, the importance of processes like stratification and turbulent mixing induced
513 by, e.g., internal wave breaking with or without sub-mesoscale coupling cannot be
514 underestimated for life near the ocean-surface as well as in the -deep, because it will come to
515 a halt without such processes.

516

517 *Data availability.* No new data were created or analyzed in this study: replot and re-analysis
518 of data presented in van Haren and Millot (2003), van Haren (2007) and van Haren (2023a).

519

520 *Competing interests.* The author declares that he has no conflict of interest.

521

522 *Acknowledgments.* I thank L. Gerringa for commenting on a previous draft of the manuscript.

523

References

Abarbanel, H. D. I., Holm, D. D., Marsden, J. E., and Ratiu, T.: Richardson number criterion
for the nonlinear stability of three-dimensional stratified flow, Phys. Rev. Lett., 52, 2352-
2355, 1984.

Albérola, C., Millot, C., and Font, J.: On the seasonal and mesoscale variabilities of the
Northern Current during the PRIMO-0 experiment in the western Mediterranean Sea,
Oceanol. Acta, 18, 163-192, 1995.

Aldama-Campino A., Fransner F., Ödalen, M., Groeskamp, S., Yool, A. Döös, K., and
Nycander, J.: Meridional ocean carbon transport, Global Biogeochem. Cy., 34
e2029GB006336, 2023.

Alford, M. H.: Redistribution of energy available for ocean mixing by long-range propagation
of internal waves, Nature, 423, 159-162, 2003.

Ashkenazi, S., and Steinberg, V.: Spectra and statistics of velocity and temperature
fluctuations in turbulent convection, Phys. Rev. Lett., 83, 4760-4763, 1999.

Bak, P., Tang, C., and Wiesenfeld, K.: Self-organized criticality: An explanation of the 1/f
noise, Phys. Rev. Lett., 59, 381-384, 1987.

Bolgiano, R.: Turbulent spectra in a stably stratified atmosphere, J. Geophys. Res., 64, 2226-
2229, 1959.

Brainerd, K. E., and Gregg, M. C.: Surface mixed and mixing layer depths, Deep-Sea Res. I,
42, 1521-1543, 1995.

Celani, A., Mazzino, A., and Vozella, L.: Rayleigh-Taylor turbulence in two dimensions,
Phys. Rev. Lett., 96, 134504, 2006.

Chini, G. P., Michel, G., Julien, K., Rocha, C. B., and Caulfield, C. P.: Exploiting self-
organized criticality in strongly stratified turbulence, J. Fluid Mech., 933, A22, 2022.

Chunchuzov, I. P., Johannessen, O. M., and Marmorino, G.O.: A possible generation
mechanism for internal waves near the edge of a submesoscale eddy, Tellus A, 73, 1-11,
2021.

551 Cisneros, M., Cacho, I., Frigola, J., Snchez-Vidal, A., Calafat, A., Pedrosa-Pàmies, R.,

552   Rumín-Caparrós, A., and Canals, M.: Deep-water formation variability in the north-

553   western Mediterranean Sea during the last 2500 yr: A proxy validation with present-day

554   data, Glob. Planet. Chang. 177, 56-68, 2019.

555 Crepon, M., Wald, L., and Monget, J. M.: Low-frequency waves in the Ligurian Sea during

556   December 1977, J. Geophys. Res., 87, 595-600, 1982.

557 Ditlevsen, P., and Ditlevsen, S.: Warning of a forthcoming collapse of the Atlantic meridional

558   overturning circulation, Nat. Comm. 14, 4254, 2023.

559 Emanuel, K., Atmospheric Convection 580 pp., Oxford Univ. Press, New York, 1984.

560 Eriksen, C. C.: Observations of internal wave reflection off sloping bottoms, J. Geophys.

561   Res., 87, 525-538, 1982.

562 Falder, M., White, N. J., and Caulfield, C. P.: Seismic imaging of rapid onset of stratified

563   turbulence in the South Atlantic Ocean, J. Phys. Oceanogr., 46, 1023-1044, 2016.

564 Ferrari, R., Mashayek, A., McDougall, T. J., Nikurashin, M. and Campin, J.-M.: Turning

565   ocean mixing upside down, J. Phys. Oceanogr., 46, 2229-2261, 2016.

566 Garrett, C.: The Mediterranean Sea as a climate test basin, In: Malanotte-Rizzoli, P., and

567   Robinson, A. R. eds., Ocean Processes in Climate Dynamics: Global and Mediterranean

568   Examples, Kluwer Academic Publishes, 227-237, 1994.

569 Garrett, C., and Munk, W.: Space-time scales of internal waves, Geophys. Fluid Dyn., 3, 225-

570   264, 1972.

571 Gascard, J.-C.: Vertical motions in a region of deep water formation, Deep-Sea Res., 20,

572   1011-1027, 1973.

573 Gascard, J-C.: Mediterranean deep water formation, baroclinic eddies and ocean eddies,

574   Oceanol. Acta, 1, 315-330, 1978.

575 Gent, P. R.: A commentary on the Atlantic meridional overturning circulation stability on

576   climate models, Ocean Mod., 122, 57-66, 2018.

Gerkema, T., Zimmerman, J. T. F., Maas, L. R. M., and van Haren, H.: Geophysical and astrophysical fluid dynamics beyond the traditional approximation, Rev. Geophys., 46, RG2004, doi:10.1029/2006RG000220, 2008.

Gou, R., Wang, Y., Xiao, K., and Wu, L.: A plausible emergence of new convection sites in the Arctic Ocean in a warming climate, Environ. Res. Lett., 19, 031001, 2024.

Gregg, M. C.: Scaling turbulent dissipation in the thermocline, J. Geophys. Res., 94, 9686-9698, 1989.

Hosegood, P., Bonnin, J., and van Haren, H.: Solibore-induced sediment resuspension in the Faeroe-Shetland Channel, Geophys. Res. Lett., 31, L09301, doi:10.1029/2004GL019544, 2004.

Kolmogorov, A. N.: The local structure of turbulence in incompressible viscous fluid for very large Reynolds numbers, Dokl. Akad. Nauk SSSR, 30, 301-305, 1941.

Kunze, E.: Near-inertial wave propagation in geostrophic shear, J. Phys. Oceanogr., 15, 544-565, 1985.

LeBlond, P. H., and Mysak, L. A.: Waves in the ocean, Elsevier, New York, 602 pp., 1978.

Lin, J.-T., Turbulence spectra in the buoyancy subrange of thermally stratified shear flows, 143 pp., PhD-thesis Colorado State University, Fort Collins, 1969.

Liot, O., Seychelles, F., Zonta, F., Chibbaro, S., Coudarchet, T., Gasteuil, Y., Pinton, J.-F., Salort, J., and Chillà, F.: Simultaneous temperature and velocity Lagrangian measurements in turbulent thermal convection, J. Fluid Mech., 794, 655-675, 2016.

Little, C. M., Zhao, M., and Buckley, M. W.: Do surface temperature indices reflect centennial-timescale trends in Atlantic Meridional Overturning Circulation strength? Geophys. Res. Lett., 47, e2020GL090888, 2020.

Liu, Z., Gu, S., Zou, S., Zhang, S., Yu, -Y., and He, C.: Wind-steered eastern pathway of the Atlantic Meridional Overturning Circulation, Nat. Geosci., 17, 353-360, 2024.

Lohse, D., and Xia, K.-Q.: Small-Scale properties of turbulent Rayleigh-Bénard convection, Annu. Rev. Fluid Mech., 42, 335-364, 2010.

604   Marotzke, J., and Scott, J. R.: Convective mixing and the thermohaline circulation, J. Phys.

605   Oceanogr., 29, 2962-2970, 1999.

606   Marshall, J., and Schott, F.: Open-ocean convection: observations, theory, and models, Rev.

607   Geophys., 37, 1-64, 1999.

608   McDougall, T. J., and Ferrari, R.: Abyssal upwelling and downwelling driven by near-

609   boundary mixing, J. Phys. Oceanogr., 47, 261-283, 2017.

610   Mertens, C., and Schott, F.: Interannual variability of deep-water formation in the

611   Northwestern Mediterranean, J. Phys. Oceanogr., 28, 1410-1424, 1998.

612   Millot, C.: Circulation in the Western Mediterranean Sea, J. Mar. Sys., 20, 423-442, 1999.

613   Munk, W.: Abyssal recipes, Deep-Sea Res., 13, 707-730, 1966.

614   Munk, W., and Wunsch, C.: Abyssal recipes II: Energetics of tidal and wind mixing, Deep-

615   Sea Res. I, 45, 1977-2010, 1998.

616   Obukhov, A. M.: Structure of the temperature field in a turbulent flow, Izv. Akad. Nauk

617   SSSR, Ser. Geogr. Geofiz., 13, 58-69, 1949.

618   Obukhov, A. M.: Effect of buoyancy forces on the structure of temperature field in a turbulent

619   flow, Dokl. Akad. Nauk SSSR, 125, 1246-1248, 1959.

620   Pawar, S. S., and Arakeri, J. H.: Kinetic energy and scalar spectra in high Rayleigh number

621   axially homogeneous buoyancy driven turbulence, Phys. Fluids, 28, 065103, 2016.

622   Perkins, H.: Observed effect of an eddy on inertial oscillations, Deep-Sea Res., 23, 1037-

623   1042, 1976.

624   Phillips, O. M.: On spectra measured in an undulating layered medium, J. Phys. Oceanogr., 1,

625   1-6, 1971.

626   Polzin, K. L., Toole, J. M., Ledwell, J. R., and Schmitt, R. W.: Spatial variability of turbulent

627   mixing in the abyssal ocean, Science, 276, 93-96, 1997.

628   Polzin, K. L., Kunze, E., Toole, J. M., and Schmitt, R. W.: The partition of finescale energy

629   into internal waves and subinertial motions, J. Phys. Oceanogr., 33, 234-248, 2003.

630   Poujade, O.: Rayleigh-Taylor turbulence is nothing like Kolmogorov turbulence in the self-

631   similar regime, Phys. Rev. Lett., 97, 185002, 2006.

Reid, R. O.: A special case of Phillips' general theory of sampling statistics for a layered medium, J. Phys. Oceanogr., 1, 61-62, 1971.

Rhein, M.: Deep water formation in the western Mediterranean, J. Geophys. Res., 100, 6943-6959, 1995.

Riley, J. J., and Lindborg, E.: Stratified turbulence: A possible interpretation of some geophysical turbulence measurements, J. Atmos Sci., 65, 2416-2424, 2008.

Saint-Guily, B.: On the response of the ocean to impulse, Tellus 24, 344-349, 1972.

Sarkar, S., and Scotti, A.: From topographic internal gravity waves to turbulence, Ann. Rev. Fluid Mech., 49, 195-220, 2017.

Schott, F., Visbeck, M., Send, U, Fischer, J., and Desaubies, Y.: Observations of deep convection in the Gulf of Lions, Northern Mediterranean, during the winter of 1991/92, J. Phys. Oceanogr., 26, 505-524, 1996.

Schuster, H. G., Deterministc Chaos: An Introduction, Physik–Verlag, Weinheim, 220 pp., 1984.

Scott, J. R., and Marotzke, J, 1998: The location of diapycnal mixing and the meridional overturning circulation, J. Phys. Oceanogr., 32, 3578-3595, 2002.

Steffen, E. L., and D'Asaro, E. A.: Deep convection in the Labrador Sea as observed by Lagrangian floats, J. Phys. Oceanogr., 32, 475-492, 2002.

Storer, B. A., Buzzicotti, M., Khatri, H., Griffies, S. M., and Aluie, H.: Global energy spectrum of the general oceanic circulation, Nat. Comm., 13, 5314, 2022.

Taira, K., Yanagimoto D., and Kitagawa, S.: Deep CTD casts in the challenger deep. Mariana Trench, J. Oceanogr., 61, 447-454, 2005.

Testor, P., and Gascard, J.C.: Post-convection spreading phase in the Northwestern Mediterranean Sea, Deep-Sea Res., 53, 869-893, 2006.

Thorpe, S. A.: Transitional phenomena and the development of turbulence in stratified fluids: a review, J. Geophys. Res., 92, 5231-5248, 1987.

Thorpe, S. A.: The turbulent ocean, Cambridge University Press, Cambridge, 439 pp, 2005.

659   van Haren, H.: Inertial and tidal shear variability above Reykjanes Ridge, Deep-Sea. Res. I,

660   54, 856-870, 2007.

661   van Haren, H.: Slow persistent mixing in the abyss, Ocean Dyn., 70, 339-352, 2020.

662   van Haren, H.: Convection and intermittency noise in water temperature near a deep

663   Mediterranean seafloor, Phys. Fluids, 35, 026604, 2023a.

664   van Haren, H.: Near-inertial wave propagation between stratified and homogeneous layers, J.

665   Oceanogr., 79, 367-377, 2023b.

666   van Haren, H.: Direct observations of general geothermal convection in deep Mediterranean

667   waters, Ocean Dyn., 73, 807-825, 2023c.

668   van Haren, H., and Dijkstra, H. A.: Convection under internal waves in an alpine lake, Env.

669   Fluid Mech., 21, 305-316, 2021.

670   van Haren, H., and Gostiaux, L.: High-resolution open-ocean temperature spectra, J.

671   Geophys. Res., 114, C05005, doi:10.1029/2008JC004967, 2009.

672   van Haren, H., and Gostiaux, L.: Detailed internal wave mixing observed above a deep-ocean

673   slope, J. Mar. Res., 70, 173-197, 2012.

674   van Haren, H. and Millot, C.: Seasonality of internal gravity waves kinetic energy spectra in

675   the Ligurian Basin, Oceanol. Acta, 26, 635-644, 2003.

676   van Haren, H., and Millot, C.: Rectilinear and circular inertial motions in the Western

677   Mediterranean Sea, Deep-Sea Res. I, 51, 1441-1455, 2004.

678   van Haren, H., Maas, L., Zimmerman, J. T. F., Ridderinkhof, H., and Malschaert, H.: Strong

679   inertial currents and marginal internal wave stability in the central North Sea, Geophys.

680   Res. Lett., 26, 2993-2996, 1999.

681   van Haren, H., Maas, L., and van Aken, H.: On the nature of internal wave spectra near a

682   continental slope, Geophys. Res. Lett., 29(12), 10.1029/2001GL014341, 2002.

683   van Haren, H., Millot, C., and Taupier-Letage, I.: Fast deep sinking in Mediterranean eddies,

684   Geophys. Res. Lett., 33, L04606, doi:10.1029/2005GL025367, 2006.

685   van Haren, H., Ribó, M., and Puig, P.: (Sub-)inertial wave boundary turbulence in the Gulf of

686   Valencia. J. Geophys. Res.Oceans, 118, 2067-2073, doi:10.1002/jgrc.20168, 2013.

van Haren, H., Uchida, H., and Yanagimoto, D.: Further correcting pressure effects on SBE911 CTD-conductivity data from hadal depths, J. Oceanogr., 77, 137-144, 2021a.

van Haren, H., Brussaard, C. P. D., Gerringa, L. J. A., van Manen, M. H., Middag, R., and Groenewegen, R.: Diapycnal mixing near the photic zone of the NE-Atlantic, Ocean Sci., 17, 301-318, 2021b.

van Haren, H., Voet, G., Alford, M. H., Fernandez-Castro, B., Naveira Garabato, A. C., Wynne-Cattanach, B. L., Mercier, H., and Messias, M.-J.: Near-slope turbulence in a Rockall canyon, Deep-Sea Res. I, 206, 104277, 2024.

van Westen, R. M., Kliphuis, M., and Dijkstra, H.A.: Physics-based early warning signal shows that AMOC is on tipping course, Sci. Adv., 10, eadk1189, 2024.

Voet, G., et al.: Near-inertial energy variability in a strong mesoscale eddy field in the Iceland Basin, Oceanogr., 37, https://doi.org/10.5670/oceanog.2024.302, 2024.

Winters, K. B.: Tidally driven mixing and dissipation in the stratified boundary layer above steep submarine topography, Geophys. Res. Lett., 42, 7123-7130, 2015.

Wunsch, C.: Gulf Stream safe if wind blows and Earth turns, Nature, 428, 601, 2004.

Wunsch, C., and Ferrari, R.: Vertical mixing, energy and the general circulation of the oceans, Ann. Rev. Fluid Mech., 36, 281-314, 2004.

Wynne-Cattanach, B. L., Couto, N., Drake, H. F., Ferrari, R., Le Boyer, A., Mercier, H., Messias, M.-J., Ruan, X., Spingys, C. P., van Haren, H., Voet, G., Polzin, K., Naveira Garabato, A., and Alford, M. H.: Observational evidence of diapycnal upwelling within a sloping submarine canyon, Nature, 630, 884-890, 2024.

Xu, Y., and Fu, L.-L.: The effects of altimeter instrument noise on the estimation of the wavenumber spectrum of sea surface height, J. Phys. Oceanogr., 42, 2229-2233, 2012.

711

712
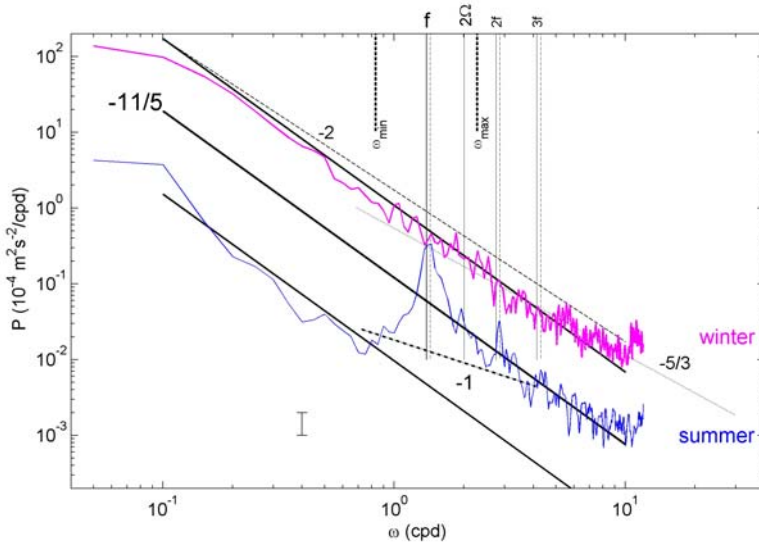
Fig. 1. Moderately smoothed (20 degrees of freedom, dof) kinetic energy (KE) spectra over 100 days of data from 3600-s sampled Aanderaa mechanical current meter moored in 1981/1982 at z = -1100 m well above the continental slope in the Ligurian Sea at 43° 28.32′ N, 7° 46.10′ E, 2250 m water depth. For details on these data, see van Haren and Millot (2003). The two spectra are not offset deliberately from each other; 'noise' also contains other signals near the Nyquist frequency. The 'summer' spectrum (blue) is an average from data between days 190 and 290 (in 1981), the 'winter' (magenta) between days 375 and 475 (adding +365 for days in 1982). Several frequencies are indicated including inertial frequency f, Earth rotational Ω and inertio-gravity wave bounds [$\omega_{min} \leq f$, $\omega_{max} \geq N, 2\Omega$] for buoyancy frequency N = f. The dashed lines indicate harmonics of 1.04f. Four spectral slopes ω^p are indicated by their exponent: p = -11/5 (solid slope in the log-log plot) for Bolgiano-Obukhov 'BO' scaling reflecting the buoyancy subrange of convection-turbulence (e.g., Pawar and Arakeri, 2016), p = -5/3 (dotted slope) for Kolmogorov-Obukhov 'KO' scaling reflecting the equilibrium inertial subrange for dominant shear-induced turbulence (Kolmogorov 1941; Obukhov, 1949), p = -1 (dash-dotted slope) for intermittency of self-organized criticality (Schuster, 1984; Bak et al., 1987) and p = -2 (dashed slope) for internal wave scaling (Garrett and Munk, 1972) or finestructure contamination (Phillips, 1971; Reid, 1971).

730
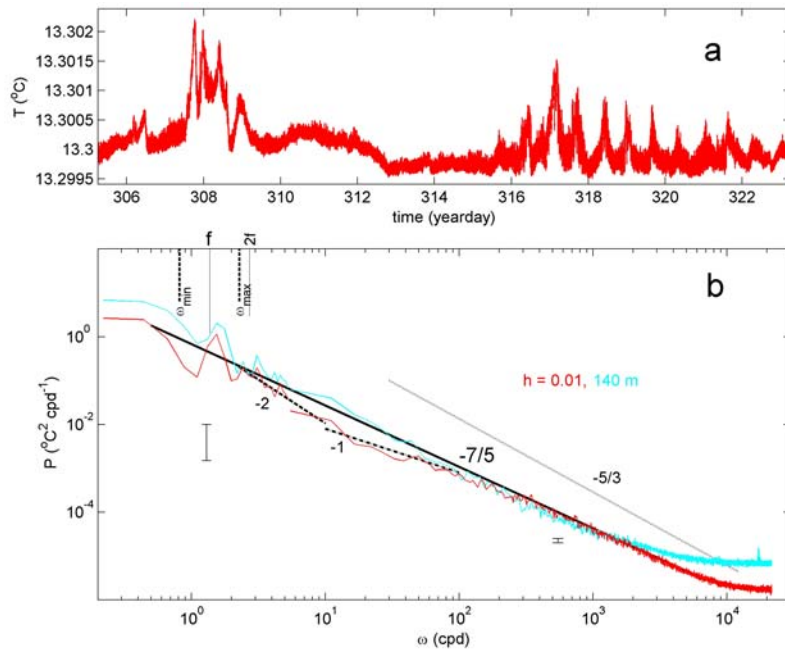
731
732 **Fig. 2**. Eighteen days of high-resolution 2-s sampled temperature 'T' data from a NIOZ

733 T-sensor fallen off a mooring-line in 2020 and lying 0.01 m above a flat seafloor about 10

734 km south of the foot of the continental slope at 42° 49.50′ N, 6° 11.78′ E, 2458 m water

735 depth, about 100 km WSW from the site in Fig. 1. For details on these data see van Haren

736 (2023a). (a) Time series of 18 days of raw temperature data. (b) Temperature variance

737 spectrum that is stitched together using two spectra with different smoothing. Weakly

738 smoothed (10 dof; ω<5 cpd) and heavily smoothed (250 dof; ω>5 cpd) spectra of data in

739 a., with bars showing the respective 95% confidence limits. For comparison, a spectrum

740 is shown in cyan from data of a less precise T-sensor at a drag-parachute line stuck at 140

741 m above the seafloor. Frequency and spectral slope indications are as in Fig. 1, while -7/5

742 (solid slope) indicates BO-scaling of an active scalar (e.g., Pawar and Arakeri, 2016).

743 Note the different axes-ranges compared with Fig. 1.
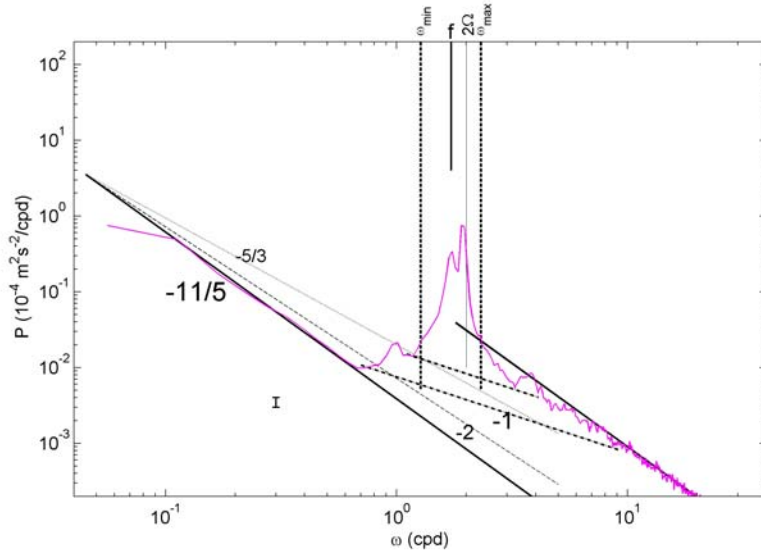
744
745 **Fig. 3**. Like Fig. 1 with the same axes ranges, but for strongly smoothed (50 dof) KE
746 spectra averaged over 400 days of data from 600-s sampled Valeport mechanical current
747 meter moored at z = -1000 m over the Mid-Atlantic Ridge at 58° 59.67′ N, 33° 56.12′ W,
748 2540 m water depth in 2003/2004, within the project discussed in van Haren (2007). The
749 small bar shows the 95% confidence interval.
750